



Research paper

High loading efficiency and sustained release of siRNA encapsulated in PLGA nanoparticles: Quality by design optimization and characterization

Dongmei Cun^{a,1}, Ditte Krohn Jensen^{a,1}, Morten Jonas Maltesen^{a,2}, Matthew Bunker^b, Paul Whiteside^b, David Scurr^c, Camilla Foged^{a,*}, Hanne Mørck Nielsen^a

^a Department of Pharmaceutics and Analytical Chemistry, University of Copenhagen, Copenhagen Ø, Denmark

^b Molecular Profiles Ltd, Nottingham, UK

^c Laboratory of Biophysics and Surface Analysis, School of Pharmacy, University of Nottingham, Nottingham, UK

ARTICLE INFO

Article history:

Received 11 August 2010

Accepted in revised form 11 November 2010

Available online 18 November 2010

Keywords:

siRNA

Poly(DL-lactide-co-glycolide acid)

Sustained release

Nanoparticles

Drug delivery

Nanomedicine

ABSTRACT

Poly(DL-lactide-co-glycolide acid) (PLGA) is an attractive polymer for delivery of biopharmaceuticals owing to its biocompatibility, biodegradability and outstanding controlled release characteristics. The purpose of this study was to understand and define optimal parameters for preparation of small interfering RNA (siRNA)-loaded PLGA nanoparticles by the double emulsion solvent evaporation method and characterize their properties. The experiments were performed according to a 2^{5-1} fractional factorial design based on five independent variables: The volume ratio between the inner water phase and the oil phase, the PLGA concentration, the sonication time, the siRNA load and the amount of acetylated bovine serum albumin (Ac-BSA) in the inner water phase added to stabilize the primary emulsion. The effects on the siRNA encapsulation efficiency and the particle size were investigated. The most important factors for obtaining an encapsulation efficiency as high as 70% were the PLGA concentration and the volume ratio whereas the size was mainly affected by the PLGA concentration. The viscosity of the oil phase was increased at high PLGA concentration, which explains the improved encapsulation by stabilization of the primary emulsion and reduction of siRNA leakage to the outer water phase. Addition of Ac-BSA increased the encapsulation efficiency at low PLGA concentrations. The PLGA matrix protected siRNA against nuclease degradation, provided a burst release of surface-localized siRNA followed by a triphasic sustained release for two months. These results enable careful understanding and definition of optimal process parameters for preparation of PLGA nanoparticles encapsulating high amounts of siRNA with immediate and long-term sustained release properties.

© 2010 Elsevier B.V. All rights reserved.

1. Introduction

The biodegradable and biocompatible polymer poly(DL-lactide-co-glycolide acid) (PLGA) has been used for decades for the

Abbreviations: Ac-BSA, acetylated bovine serum albumin; AFM, atomic force microscopy; ANOVA, analysis of variance; DCM, dichloromethane; DEPC, diethyl pyrocarbonate; DOE, design of experiments; DOTAP, dioleoyltrimethylammonium-propane; EGFP, enhanced green fluorescent protein; FBS, fetal bovine serum; FDA, Food and Drug Administration; FFD, fractional factorial design; FLuc, firefly luciferase; LF, lipofectamine; PBS, phosphate-buffered saline; PCS, photon correlation spectroscopy; PDI, polydispersity index; PEI, polyethyleneimine; PLGA, poly(DL-lactide-co-glycolide acid); PVA, polyvinylalcohol; siRNA, small interfering RNA; ToF-SIMS, time-of-flight secondary ion mass spectrometry.

* Corresponding author. Faculty of Pharmaceutical Sciences, Department of Pharmaceutics and Analytical Chemistry, University of Copenhagen, Universitetsparken 2, DK-2100 Copenhagen Ø, Denmark. Tel.: +45 35 33 64 02; fax: +45 35 33 60 01.

E-mail address: cfo@farma.ku.dk (C. Foged).

¹ These authors contributed equally.

² Present address: Novo Nordisk A/S, Novo Nordisk Park, DK-2760 Måløv, Denmark.

delivery of a variety of drug molecules including small molecular weight compounds, peptides and proteins [1,2]. It is approved for human use by the Food and Drug Administration (FDA), and several PLGA-based formulations have received worldwide marketing approval [3,4]. The polymer has also caught interest for the delivery of nucleic acids like small interfering RNA (siRNA), and there is an increasing enthusiasm for exploring matrix systems like PLGA-based particles for siRNA delivery as an alternative to commonly used cationic and/or non-biodegradable gene delivery systems to avoid toxicity associated with these [5,6]. In particular, PLGA nanoparticles have attracted much attention since they are assumed to meet the criteria required for successful siRNA delivery: (i) They are sufficiently small for efficient tissue penetration and cellular uptake, (ii) the siRNA can be entrapped into the PLGA matrix, which offers physical protection against RNase activity as well as a favorable colloidal stability of the system, and (iii) the PLGA particles generally possess an excellent controllable and alterable degradation profile and thus drug release span from days to years

depending on the molecular weight, the composition of the block copolymer and the structure of the nanoparticles [6].

Previous reports have shown that PLGA nanoparticles are safe and efficient carriers for the delivery of plasmid DNA [7,8]. However, from a technical point of view, it is difficult to load smaller nucleic acid molecules like siRNA into PLGA nanoparticles obtaining a high loading and encapsulation efficiency with the use of the classical preparation methods like the double emulsion solvent evaporation method. As other low molecular weight compounds, siRNA easily leaks from the inner water phase into the outer water phase during preparation due to its relatively low molecular weight, its hydrophilic character and the electrostatic repulsion forces present between the phosphate groups in the siRNA backbone and the anionic acid groups in the PLGA polymer. As a result, siRNA is usually incorporated into the PLGA nanoparticles with very low encapsulation efficiency and a limited loading percent, which represents a significant bottleneck for the further development of PLGA nanoparticles for siRNA delivery.

A common strategy to increase the loading is to complex siRNA with cationic excipients like dioleoyltrimethylammoniumpropane (DOTAP) [9], polyethyleneimine (PEI) [10] or polyamines [11] to enhance the affinity between the siRNA and the particle matrix, thereby increasing the loading percent and the encapsulation efficiency of siRNA. However, such cationic excipients are often associated with toxicity and can retard the release of siRNA. It is therefore relevant to optimize the loading by other means and of ultimate importance to systematically investigate the effects of formulation and process parameters on the siRNA encapsulation efficiency into PLGA nanoparticles, since it has been shown that certain formulation and process variables significantly affect the encapsulation efficiency of macromolecular drugs into PLGA particles [12–14].

Design of experiments (DOE) is an efficient method for evaluating the effects of formulation and process parameters on response variables, and for subsequent optimization of these parameters with respect to the final specifications [15,16]. Therefore, DOE is commonly adopted in pharmaceutical research since it provides the possibility of obtaining maximal information from a minimal number of experiments.

In the current study, siRNA-loaded PLGA nanoparticles were prepared by the double emulsion solvent evaporation technique [17]. The formulation and preparation process parameters were rationally optimized by a thorough understanding of the effect of various parameters including (i) the volume ratio between the inner water phase and the oil phase, (ii) the PLGA concentration, (iii) the sonication time for the primary emulsification, (iv) the siRNA load and (v) the amount of acetylated bovine serum albumin (Ac-BSA) added to the inner water phase to stabilize the primary emulsion. The experiments were planned by DOE, and parameters were optimized with respect to high siRNA loading percent and encapsulation efficiency without compromising the particle size. The optimal formulations were used to study the *in vitro* release behavior of siRNA from the PLGA nanoparticles, the surface composition of the nanoparticles by time-of-flight secondary ion mass spectrometry (ToF-SIMS), the protection achieved against nucleases, and finally the biological activity of the encapsulated siRNA.

2. Materials and methods

2.1. Materials

Enhanced green fluorescent protein (EGFP) and firefly luciferase (FLuc) Dicer substrate asymmetric duplex siRNAs were provided by Integrated DNA Technologies BVBA (Leuven, Belgium) as dried, annealed, purified and desalted duplexes. Sequences were as follows: EGFP, sense 5'-pACCCUGAAGUUAUCUGCACACcg-3',

antisense 5'-CGGUGGUGCAGAUGAACUUCAGGGUCA-3', FLuc sense 5'-pGGUUCUGGAACAAUUGCUUUUAca-3', antisense 5'-UGUAAAAGCAAUUGUCCAGGAACCAG-3' [10]. Lower case letters are 2'-deoxyribonucleotides and underlined capital letters are 2'-O-methylribonucleotides. Cy3-labeled siRNA was purchased from Dharmacon Research (Lafayette, CO, USA) as dried 2'-hydroxyl, annealed, purified and desalted duplexes. Sequences were as follows: Cy3-EGFP, sense 5'-GACGUAAACGGCCACAAGUUC-3', antisense 5'-ACUUGUGCCGGUUUACGUCGC-3'. PLGA (lactide:glycolide molar ratio of 75:25, Mw: 20 kDa) was purchased from Wako Pure Chemical Industries, Ltd. (Osaka, Japan). Polyvinylalcohol (PVA) 403 with an 80.0% degree of hydrolysis was provided by Kuraray (Osaka, Japan). Ac-BSA was obtained from Sigma Chemical Co. (St. Louis, MO, USA). Quant-iT™ RiboGreen® RNA Reagent and SYBR® Green II RNA gel stain were purchased from Molecular Probes Ltd., Invitrogen (Paisley, UK). All other general chemicals and reagents were obtained commercially at analytical grade.

2.2. Preparation of siRNA-loaded PLGA nanoparticles

The siRNA-loaded PLGA nanoparticles were prepared by the water-in-oil-in-water ($w_1/o/w_2$) double emulsion solvent evaporation method as previously reported [17]. In brief, a solution of siRNA in TE buffer (10 mM Tris-HCl and 1 mM EDTA in MilliQ water, pH 7.5) with or without Ac-BSA was mixed with dichloromethane (DCM) containing various amounts of PLGA, and the mixture was emulsified by sonication using a UP100H ultrasonic processor (Hielscher Ultrasonics GmbH, Teltow, Germany) into a primary w_1/o emulsion. Two ml of 2% (w/v) PVA in MilliQ water was poured directly into the primary emulsion and further emulsified by sonication for another 60 s to form a $w_1/o/w_2$ double emulsion. The resulting emulsion was diluted with 6 ml of 2% (w/v) PVA in MilliQ water and stirred magnetically for 3 h at room temperature to evaporate the DCM. The PLGA nanoparticles were collected by ultracentrifugation (Optima™ Max Ultracentrifuge, Beckman COULTER, CA, USA) at 38,000g for 10 min at 4 °C, washed twice with 6 ml of diethyl pyrocarbonate (DEPC) treated water, re-suspended in DEPC-treated water, and freeze-dried as described previously [17].

2.3. Experimental design

A 2^{5-1} fractional factorial design (FFD) was created in SAS-JMP 7.0 (SAS institute Inc., Cary, NC, USA) to determine the effect of process parameters on the particle characteristics. The chosen independent process parameters were the volume ratio between the inner water phase and the oil phase (X_1), the PLGA concentration (X_2), the sonication time for the primary emulsification (X_3), the siRNA load (X_4) and the Ac-BSA content in the inner water phase (X_5). These parameters were chosen based on results from previous experiments [17]. Each process parameter was studied at the two levels listed in Table 1.

The levels were chosen to provide a maximal design space and still enable feasible processing of the particles. In addition, two centre points were included to evaluate the curvature of the statistical model. All runs of the experimental design were randomised to eliminate biased variance. Two response variables (dependent variables) were analyzed including the encapsulation efficiency of the siRNA (Y_1) and the particle size (Y_2). Each measurement was conducted in triplicate. An overview of the experimental design including the results is given in Table 2.

The applied experimental design is of resolution V, which means that the main effects are confounded with four-factor interactions, and two-factor interactions are confounded with three-factor interactions. Interaction terms indicate that the effect on a response variable produced by changing one parameter level

Table 1
Process and formulation parameters addressed in the fractional factorial design.

Parameter	Component	Units	Applied levels		
			Low level	Center level	High level
X_1	V_{w1}/V_o	ratio	0.1	0.3	0.5
X_2	C_{PLGA}	mg/ml	20.0	40.0	60.0
X_3	$t_{sonication}$	sec	30.0	60.0	90.0
X_4	m_{siRNA}	μ g	35.9	62.8	89.7
X_5	m_{Ac-BSA}	mg	0.0	200	400

depends on the level of the other parameter present in the interaction term. The main effects and the two-factor interactions are included in the statistical model given in Eq. (1):

$$Y = \beta_0 + \sum \beta_i X_i + \sum \beta_{ij} X_i X_j + \varepsilon \quad (1)$$

where Y is the predicted response, β is the parameter estimate, X is the coded value of the independent parameter and ε is the residual error. The effect and significance of the main factors and the two-factor interactions were evaluated by analysis of variance (ANOVA), where the statistical models for the different dependent variables were fitted independently. The coefficients in Eq. (1) were calculated using coded values of the independent parameters according to Eq. (2):

$$x_i = \frac{X_i - (X_{i,high} + X_{i,low})/2}{(X_{i,high} - X_{i,low})/2} \quad (2)$$

where x_i is the coded value of the natural independent variable X_i , and $X_{i,high}$ and $X_{i,low}$ are the high and low levels of the variable. Instead of the actual values, the coding results in a value of -1 for the low levels and a value of $+1$ for the high levels. As a result, positive coefficients mean that the output increases with an increase in parameter level, and negative coefficients that the output increases with a decrease in parameter level. Statistical models were accepted when there was no lack of fit, no correlation in the residual plots and the residuals were normally distributed.

2.4. Characterization of nanoparticles

Freeze-dried nanoparticles were re-dispersed in DEPC-treated water (0.2 mg/ml) by a short period of gentle sonication

(<1 min). The mean particle diameter (Z-average) and polydispersity index (PDI) were determined by dynamic light scattering using the photon correlation spectroscopy (PCS) technique. The zeta potential was measured by the laser Doppler electrophoresis technique. The measurements were performed on undiluted samples ($n = 3$) in DEPC-treated water at 25 °C using a Malvern NanoZS (Malvern Instruments Ltd., Worcestershire, UK) equipped with a 633-nm laser and 173° detection optics. The voltage used for the zeta potential measurements was selected automatically based on the measured conductivity of the sample. The Helmholtz–Smoluchowski equation was used to convert the electrophoretic mobility to the zeta potential. Malvern DTS v.5.00 software (Malvern Instruments Ltd., Worcestershire, UK) was used for data acquisition and analysis. A polystyrene particle size standard (220 ± 6 nm, Duke Scientific Corp., NC, USA) and zeta potential transfer standard ($-50 \text{ mV} \pm 5 \text{ mV}$, Malvern Instruments Ltd.,) were used to verify the performance of the instrument.

The surface morphology of the nanoparticles was studied by atomic force microscopy (AFM). Samples were prepared by dispersing freeze-dried particles in de-ionized water by sonication. A drop of the resulting suspension was placed onto a nucleopore 0.1- μ m filter (Agar Scientific, Stanstead, UK) and left until the liquid had evaporated. Images were recorded using tapping mode in air on a MultiMode Nanoscope IIIa instrument equipped with a J-scanner (Veeco Instruments, Santa Barbara, USA) and Tap300 probes (Budget Sensors, Sofia, Bulgaria).

The siRNA encapsulation efficiency was determined by measuring the amount of extractable siRNA in the freeze-dried PLGA nanoparticles. For each sample, 2 mg of freeze-dried nanoparticles was dissolved in 200 μ l of chloroform, and 500 μ l of TE buffer was added. The mixture was rotated end-over-end for 90 min at room temperature to facilitate extraction of siRNA from the organic phase into the aqueous phase. The aqueous and organic phases were separated by centrifugation for 20 min at 18,000g at 4 °C (refrigerated centrifuge SIGMA 1-15PK, Osterode am Harz, Germany). The supernatant was collected and incubated at 37 °C for 5 min to remove residual chloroform. The samples were then further diluted with TE buffer, and the siRNA concentration was measured by the RiboGreen® RNA reagent according to the manufacturer's instructions using a FLUOstar OPTIMA plate reader (BMG Labtech GmbH, Offenburg, Germany) at an excitation wavelength

Table 2
Experimental design and results.

Run No.	Coded independent parameters					Dependent parameters	
	X_1	X_2	X_3	X_4	X_5	Y_1^a (%)	Y_2^a (nm)
1	–	+	–	–	–	33.25 ± 10.98	244.6 ± 0.8
2	–	+	+	+	–	9.95 ± 0.84	248.0 ± 4.1
3	–	–	+	+	+	23.15 ± 2.45	221.2 ± 1.7
4	+	–	–	+	+	23.09 ± 2.91	225.5 ± 1.1
5	+	+	–	+	–	49.69 ± 1.68	256.2 ± 4.0
6	+	+	–	–	+	42.29 ± 1.91	252.6 ± 2.7
7	–	–	–	–	+	21.86 ± 4.18	218.3 ± 0.7
8	0	0	0	0	0	33.72 ± 1.95	241.7 ± 2.0
9	+	–	–	–	–	3.03 ± 0.17	232.4 ± 1.4
10	–	–	–	+	–	2.01 ± 0.65	225.8 ± 2.9
11	0	0	0	0	0	32.97 ± 2.66	230.9 ± 1.7
12	–	+	+	–	+	31.86 ± 1.78	250.6 ± 1.7
13	+	–	+	+	–	7.77 ± 0.05	242.6 ± 1.3
14	–	+	–	+	+	14.59 ± 0.64	255.6 ± 1.6
15	+	+	+	+	+	51.18 ± 4.65	256.2 ± 2.1
16	–	–	+	–	–	6.16 ± 1.38	227.9 ± 3.1
17	+	+	+	–	–	44.86 ± 1.39	257.9 ± 2.7
18	+	–	+	–	+	31.92 ± 2.75	222.8 ± 1.7

+ High level.

– Low level.

0 Center level.

^a Values represent mean ± SD ($n = 3$).

of 485 nm and an emission wavelength of 520 nm. Each sample was assayed in triplicate. The siRNA loading and encapsulation efficiency were calculated using the following Eqs. (3) and (4):

$$\text{siRNA loading} = \frac{\text{the weight of drug in nanospheres (ng)}}{\text{the weight of nanospheres (mg)}} \quad (3)$$

$$\text{encapsulation efficiency} = \frac{\text{actual siRNA loading}}{\text{theoretical siRNA loading}} \times 100\% \quad (4)$$

2.5. Viscosity of oil phase

The viscosity of PLGA in DCM was evaluated using an AR-G2 rheometer (TA Instruments, Crawley, UK) equipped with a double gap peltier cylinder system and a double gap rotor for a concentric cylinder system in order to minimize evaporation during the measurements. The viscosity was measured at 25 °C at a shear rate gradient between 1 s⁻¹ and 600 s⁻¹. For each shear rate, an average of three measurements of 10 s was used.

2.6. Release of siRNA

The release of siRNA was measured in TE buffer using PLGA nanoparticles loaded with Cy3-labelled siRNA. Briefly, 2.0 mg of freeze-dried nanoparticles was suspended in 0.5 ml TE buffer in RNase-free Eppendorf tubes and shaken in a water bath (50 rpm) at 37 °C. At given times (after 2 and 6 h at day 0, once a day for the first four days and thereafter every second day), the tubes were centrifuged (18,000g for 15 min), the supernatants were collected for analysis, and the nanoparticle deposits were re-dispersed in fresh TE buffer to avoid PLGA degradation-dependent changes in the buffer pH and re-incubated. Samples were taken and analyzed in triplicates. The concentration of released Cy3-siRNA was measured using the FLUOstar OPTIMA plate reader at an excitation wavelength of 544 nm and an emission wavelength of 590 nm. The percentage of released siRNA was normalized to the total recovered amount of siRNA.

2.7. Time-of-flight secondary ion mass spectrometry

The presence of siRNA on the surface of the nanoparticles was analyzed using ToF-SIMS. Freeze-dried samples were adhered to double-sided tape to produce a surface suitable for ToF-SIMS analysis. Spectra were recorded using an ToF-SIMS IV instrument (ION-TOF GmbH, Münster, Germany) equipped with a Bi₃⁺ primary ion source, providing a mass resolution of >1:10,000. Each sample was raster-scanned to ensure representative analysis over areas of approximately 10–30 μm at a resolution of 256 × 256 pixels. A low energy electron flood gun was used to charge compensate the insulating nature of the sample. The total primary ion beam dose for every analyzed area was kept below 1 × 10¹² ions/cm² throughout the analysis, ensuring static conditions.

2.8. RNase protection assay

Nanoparticles corresponding to an siRNA load of 670 ng of siRNA were dispersed in 10 μl of acetate buffer (50 mM, pH 5.0) and incubated with 5 ng/μl of Ribonuclease I “A” (bovine pancreas) (GE healthcare, Hillerød, Denmark) test solution at 37 °C. The reaction was terminated at 1, 24, 72, 96 and 120 h by the addition of 2 μl 120 mM EDTA solution, and the samples were frozen at -80 °C until further analysis. The particles were then collected by ultracentrifugation (18,000g for 12 min at 4 °C), washed with DEPC-water, and the siRNA was recovered by TE buffer/chloroform

extraction. A volume of the buffer layer containing extracted siRNA was concentrated by the use of a microcon[®] centrifugal filter device YM-3 with a cut-off size of 3000 Da (Millipore, Billerica, MA, USA) at 14,000g and 4 °C. The integrity of the siRNA was analyzed on a 4–20% polyacrylamide gel (PAGER Gold, Lonza, Basel, Switzerland) using TBE buffer (0.089 M Tris base, 0.089 M boric acid, and 2 mM sodium EDTA in MilliQ water, pH 8.3, Bio-Rad Laboratories, Copenhagen, Denmark) at a constant voltage of 100 V for 1 h. The siRNA bands were visualized using an image station (Kodak Image Station 1000, Eastman Kodak Company, OR, US) after staining for 40 min with a 1:10,000 dilution of SYBR-Green II RNA gel stain prepared in DEPC-treated water. For comparison, 400 ng of free siRNA in 10 μl acetate buffer (50 mM, pH 5.0) was incubated under similar conditions and analyzed on the gel after termination of the RNase reaction (1, 24 and 72 h).

2.9. Biological activity of siRNA in PLGA nanoparticles

The biological activity of the extracted siRNA was examined essentially as described previously [18] by transfection of EGFP-expressing H1299 cells using the commercial transfection reagent lipofectamine 2000 (Invitrogen A/S, Taastrup, Denmark).

2.9.1. Cell culture

H1299 cells stably expressing EGFP were maintained in RPMI 1640 Medium (Fisher Scientific Biotech Line, Slangerup, Denmark) supplemented with 100 U/ml penicillin, 100 μg/ml streptomycin, 2 mM L-glutamine (all from Sigma-Aldrich, Brøndby, Denmark), 0.2 mg/ml Geneticin (Invitrogen A/S, Taastrup, Denmark) and 10% (v/v) fetal bovine serum (FBS) (PAA Laboratories GmbH, Pasching, Austria). The cells were grown in an atmosphere of 5% CO₂/95% O₂ at 37 °C, the growth medium was replaced every 48 h, and the cells were sub-cultured approximately 1:5 twice a week. The cells were detached from the culture flasks by incubating the cells for 5 min at 37 °C with TrypLE[™] Express (Invitrogen A/S, Taastrup, Denmark). Prior to siRNA addition, the cells were seeded in 24-well tissue culture plates in 0.5 ml growth medium, at a density of 8 × 10⁴ cells per well, and kept at normal culturing conditions for 24 h.

2.9.2. Biological activity of siRNA extracted from PLGA nanoparticles

After 24 h (and at approximately 80% confluency), the cells were incubated with 300 μl of pre-mixed samples in RPMI 1640 medium containing 10% (v/v) FBS for 48 h at 37 °C. The siRNA from stock solution or extracted from the nanoparticles was combined with Lipofectamine 2000 in amounts recommended by the manufacturer and added to the H1299 cells at a concentration of 2 nM siRNA. After incubation, the cells were washed with 500 μl phosphate-buffered saline (PBS), and 100 μl of TrypLE 336 TM Express (Invitrogen A/S, Taastrup, Denmark) was added. After incubation for 5 min, 1 ml of growth medium was added, the cells were transferred to tubes and centrifuged (10 min, 1076g, 4 °C). The supernatant was removed, and the cells were re-dispersed in PBS containing 10% (v/v) FBS followed by a second centrifugation, after which the cells were re-dispersed in 0.5 ml ice-cold PBS containing 10% (v/v) FBS and 1 μg/ml propidium iodide (PI) (Invitrogen A/S, Taastrup, Denmark) for staining of dead cells. The cells were analyzed on a FACScan flow cytometer (Becton Dickinson, NJ, USA) using the CellQuest Software (Becton Dickinson). Dead cells were excluded based on the PI-staining.

3. Results

3.1. Optimization of the siRNA-loaded PLGA nanoparticle formulation

The purpose of the FFD was to identify parameters that have a significant effect on the analyzed response variables. The choice

Table 3
Results of the fractional factorial design.

Parameter	Y ₁		Y ₂	
	Estimate (β)	t-Ratio	Estimate (β)	t-Ratio
X ₁	12.30	8.12	3.39	3.18
X ₂	19.84	9.26	25.65	12.04
X ₃	1.07 ^a	0.99		
X ₄	-2.11	-1.97		
X ₅	0.27	0.18	1.04	0.69
X ₁ *X ₂	10.72	5.01		
X ₁ *X ₃				
X ₁ *X ₄	3.32	3.10		
X ₁ *X ₅				
X ₂ *X ₃				
X ₂ *X ₄				
X ₂ *X ₅	-9.86	-4.61	6.15	2.89
X ₃ *X ₄				
X ₃ *X ₅	3.47	3.24		
X ₄ *X ₅				
R-value	0.97		0.93	

^a Parameter t-ratios in italic are not significant but are present in the interaction parameters and therefore included in the model.

of the five process parameters was based on previous experiments [17]. The response parameters were the siRNA encapsulation efficiency and the particle size.

3.1.1. Encapsulation efficiency

The encapsulation efficiency of a drug into a nanoparticulate drug delivery system is one of the most important dependent variables, and the ability to control this is crucial. The aim of this study was to maximize the encapsulation efficiency (Y₁) of the siRNA in the nanoparticles. The measured encapsulation efficiency ranged from 2.01% to as much as 51.18% (Table 2) depending on the process parameters yielding a rather complex statistical model with two significant main effects and four significant interaction terms describing 0.97 of the variation (Table 3).

The most significant process parameter explaining the variation in the encapsulation efficiency was the PLGA concentration (X₂, β 19.84), followed by the volume ratio (X₁, β 12.30). Both the PLGA concentration and the volume ratio are positively correlated

with the encapsulation efficiency meaning that an increase in one of these parameters causes an increase in the encapsulation efficiency of the siRNA (Table 3). The PLGA concentration and the volume ratio were the only significant main effects. However, all five parameters were part of a significant interaction term and thus all tested main effects should be included in the statistical model describing the encapsulation efficiency (Table 3). The level of significance of the PLGA concentration suggests a direct interaction between the PLGA and the siRNA, which affects the encapsulation efficiency of the siRNA. Surprisingly, the siRNA load does not contribute significantly to the encapsulation efficiency and it is only present in one of the interaction terms with a smaller impact. An interaction is however evident between the siRNA load and the ratio between the organic phase and the inner water phase (X₁*X₄). Since the ratio between the inner water phase and the organic phase was varied by changing the volume of the inner water phase, it essentially corresponds to variations in the siRNA concentration which thus seems to exert a significant effect on the encapsulation efficiency. More information on the effect of the siRNA load on encapsulation efficiency could perhaps be obtained by testing at a wider range of siRNA loads. The content of Ac-BSA in the inner water phase did not exert a significant direct effect on the encapsulation efficiency, but was included in a significant two-factor interaction with the PLGA concentration (X₂*X₅). The described two-factor interaction between the PLGA concentration and the Ac-BSA content shows that there is a positive effect of including Ac-BSA in the formulation at low PLGA concentrations, whereas the effect is absent at high PLGA concentrations (Fig. 1).

A relatively large interaction is also observable between the ratio of the inner water phase to the organic phase and the PLGA concentration (X₁*X₂) revealing a positive synergistic effect between the two factors. The final interaction term between the sonication time and the BSA content (X₃*X₅) might indicate that a longer sonication time is necessary for obtaining a homogeneous emulsion when BSA is included in the inner water phase (Fig. 1).

3.1.2. Size

The particle size is an important physical parameter for particulate drug delivery systems. Prior to the experiments,

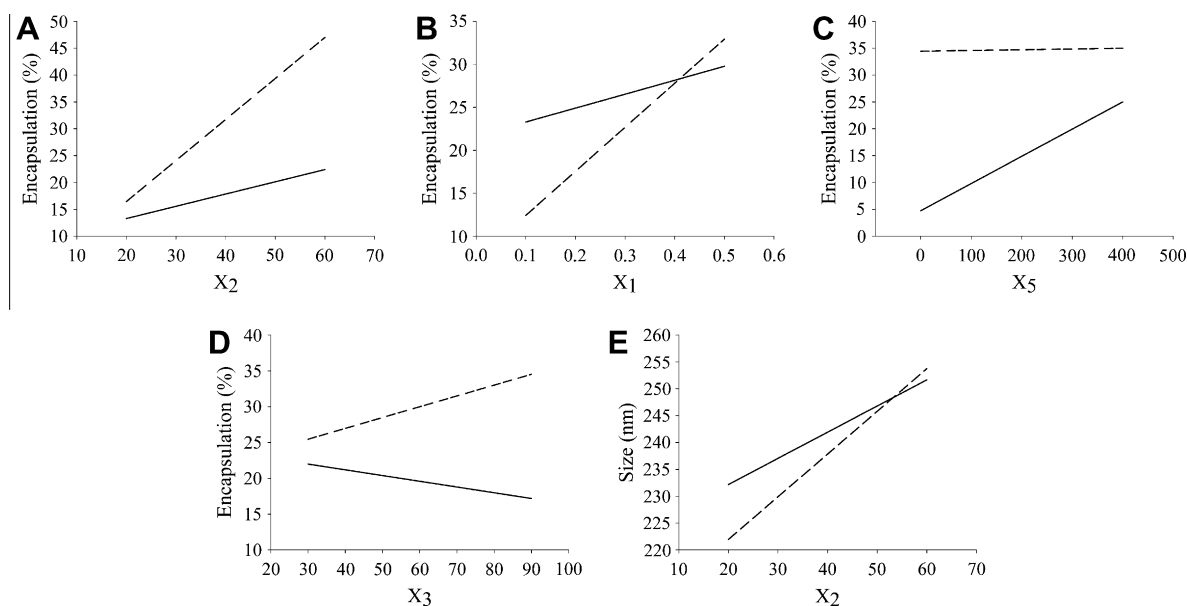


Fig. 1. Interaction plots showing significant two-way interaction terms for the dependent variables. Solid lines display factor at low level, whereas dashed lines are the high level of the factors. A: interaction term X₁X₂ – Volume ratio/PLGA concentration. B: X₁X₄ – Volume ratio/siRNA load. C: X₂X₅ PLGA concentration/Ac-BSA content. D: X₃X₅ – Sonication time/Ac-BSA content. E: X₂X₅ – PLGA concentration/Ac-BSA content. A–D: Encapsulation efficiency. E: particle size.

Table 4
Optimal parameters for formulation of siRNA-loaded PLGA nanoparticles.

	Low siRNA load	High siRNA load
$m_{\text{PLGA}(7520)}$	30 mg	30 mg
CH_2Cl_2	0.5 ml	0.5 ml
m_{siRNA}	36 μg	90 μg
$m_{\text{Ac-BSA}}$	400 μg	400 μg
$V_{\text{TE buffer}}$	230 μl	200 μl
$V_{2\% \text{ PVA}}$	2 + 6 ml	2 + 6 ml
siRNA load ^a	770 \pm 33 ng/mg nanoparticles	2192 \pm 115 ng/mg nanoparticles
EE ^a	64.35 \pm 2.78%	70.63 \pm 5.75%
Yield	92.0%	91.0%
Z-average ^a	256.0 \pm 3.0 nm	265.2 \pm 1.8 nm

^a Values represent mean \pm SD ($n = 3$).

300 nm was pre-defined as the maximal acceptable diameter for the nanoparticles. The particle size of the produced nanoparticles ranged from 218.3 nm to 257.9 nm (Table 2), and thus, all experiments yielded particle sizes in the desired range. However, the particle size dependency on the process parameters is still important and crucial for the understanding of the preparation of siRNA-loaded nanoparticles. As for the encapsulation efficiency, the most significant parameter for describing the variation in the particle size (Y_2) was the PLGA concentration (X_2 , $\beta_{25.65}$) followed by the volume ratio (X_1 , $\beta_{3.39}$) and the interaction term between the PLGA concentration and the Ac-BSA concentration ($X_2 * X_5$, $\beta_{6.15}$) (Table 3). The variation explained by the statistical model was 0.93. All significant parameters were positively correlated with the particle size meaning that an increase in parameter level increased the particle size. The zeta potential of the particles were all negative and in the range of -45.5 mV to -37.5 mV (results not shown).

3.1.3. Optimal parameters for the formulation of siRNA-loaded PLGA nanoparticles

Based on the above-mentioned experiments, optimal parameters were identified for the preparation of two different siRNA-loaded PLGA nanoparticle formulations (Table 4), one with a low siRNA load (770 \pm 33 ng/mg nanoparticles) and one with a high siRNA load (2192 \pm 115 ng/mg nanoparticles). For the optimized batches, the encapsulation efficiencies were 64.35 \pm 2.78 % and 70.63 \pm 5.75 %, and the average particle sizes were 256.0 \pm 3.0 nm and 265.2 \pm 1.8 nm, respectively. Example AFM topography images of nanoparticles with a high siRNA load are displayed in Fig. 2. The nanoparticles are spherical in shape and show smooth, featureless

surfaces. The nanoparticles show an approximate range of diameters between 100 and 600 nm with an average of 200 nm. It should be noted that the AFM probe shape and the packing of the nanoparticles have an influence on the measured radius from AFM images.

3.2. Sustained release of siRNA from the polymeric matrix

To describe and compare the release kinetics of siRNA from the nanoparticles prepared by the optimal parameters, the release of Cy3-labelled siRNA from the PLGA nanoparticles was determined in TE buffer. The release profile is characterized by an initial and fast burst release of 12–15% of the encapsulated siRNA (Fig. 3), followed by a lag-time lasting for approximately four days. Thereafter, the siRNA was released at a constant rate in two phases, the first phase lasting until around day 20, whereafter the siRNA was released at a slower but still constant rate. After 54 days, approximately 60% of the total recovered amount of siRNA was released from the matrix, whereas 40% was still retained in the PLGA matrix. Due to the frequent buffer change, the buffer pH remained constant during the incubation period (results not shown).

3.3. siRNA is present on the surface of the nanoparticles

To evaluate whether siRNA localized at the surface of the nanoparticles, ToF-SIMS spectra were recorded from an siRNA reference sample, non-loaded, placebo nanoparticles and nanoparticles with a high siRNA load. An overview of the negative ion spectra for the siRNA reference material and the placebo formulation is presented in Fig. 4. Close inspection of the spectra permits identification of peaks directly attributable to the nitrogen-containing bases present in the siRNA molecules [19]: 110.03 m/z ($\text{C}_4\text{H}_4\text{N}_3\text{O}$); 125.03 m/z ($\text{C}_5\text{H}_5\text{N}_2\text{O}_2$) and 150.02 m/z ($\text{C}_5\text{H}_4\text{N}_5\text{O}$). In addition, 62.96 m/z (PO_2^-) and 78.96 (PO_3^-) ion fragments originating from the phosphate backbone are also highlighted as suitable indicators.

The fragment ions originating from the siRNA base groups were not observed in the ToF-SIMS spectrum acquired from the siRNA-loaded PLGA nanoparticles. This can be explained as being due to the fact that the surface-loading of siRNA is believed to be very low, such that the corresponding ion fragment are below the sensitivity of the instrument. In contrast, the peaks assigned to the PO_2^- and PO_3^- ion fragments were observed above the background noise (Fig. 5). Therefore, these fragments were selected as indicators to confirm the presence of siRNA at the surface of the siRNA-loaded nanoparticles. A comparison with the placebo, non-loaded PLGA nanoparticles was made to provide a control.

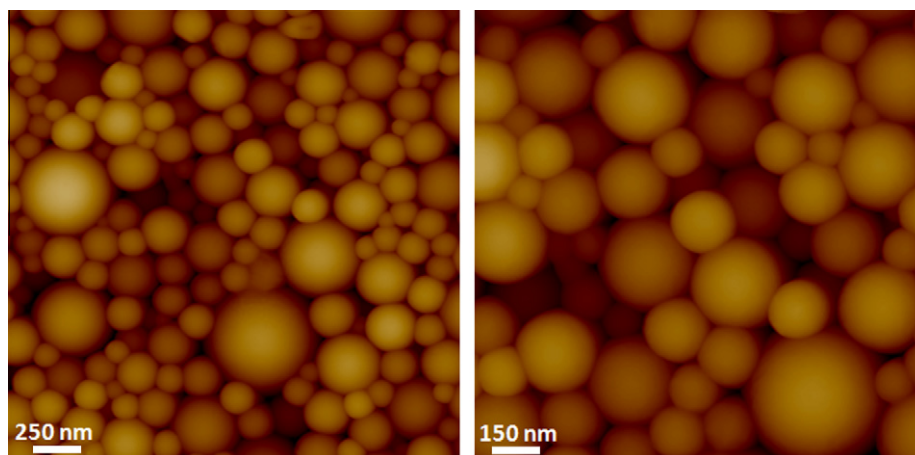


Fig. 2. AFM topography images of siRNA-loaded nanoparticles at two different scan sizes.

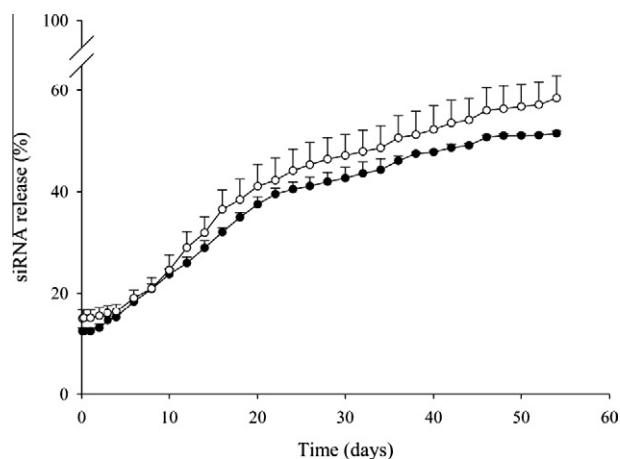


Fig. 3. Release of siRNA from different batches of PLGA nanoparticles with two different siRNA loadings. *Open circles*: High loading of siRNA (2192 ± 115 ng/mg nanoparticles). *Filled circles*: Low loading of siRNA (770 ± 33 ng/mg nanoparticles). Data points represent mean \pm SD ($n = 3$).

Closer inspection of the ToF-SIMS spectra in the regions of interest is shown in Figs. 5 and 6. A peak at 62.96 m/z in the siRNA-loaded PLGA nanoparticles is present in Fig. 5a, which is absent in the placebo (Fig. 5c). Similar inspection of Fig. 6, and the peak at 78.96 m/z, provides a consistent result and conclusion. These findings suggest the presence of some siRNA at the surface of the siRNA-loaded PLGA nanoparticles.

3.4. The polymeric matrix protects siRNA from degradation by RNase

To evaluate the ability of the PLGA matrix to protect the siRNA from nuclease activity, siRNA-loaded nanoparticles were incubated with Ribonuclease I "A". The PLGA matrix was able to protect the siRNA against degradation for up to 120 h (Fig. 7), whereas most of the naked siRNA was degraded within an hour of incubation with Ribonuclease. This suggests that the polymeric matrix can protect the siRNA from degradation.

3.5. The biological activity of siRNA is preserved during the nanoparticle preparation process

To show that the biological activity of the siRNA was preserved during the preparation process, the siRNA directed against the mRNA encoding EGFP was extracted from the nanoparticles and used in gene silencing experiments in H1299 cells stably transfected with EGFP. The extracted siRNA was as efficient as the positive control siRNA in silencing the EGFP expression (Fig. 8). The above results show that the functional properties of the siRNA are not affected by the nanoparticle preparation procedure.

4. Discussion

A successful nanoparticulate delivery system should, apart from possessing a favorable safety profile, have a high loading capacity in order to reduce the quantity of both the drug and the excipient material to be used for therapy. This is in particular important for costly biopharmaceuticals like siRNA. As the main validation parameter in the present study was the encapsulation efficiency of the siRNA, focus was on the process variables relevant for the formation and stabilization of the first emulsion, i.e. the primary water phase and oil phase.

The results of the present FFD study show that even though the PLGA concentration and the w_1/o volume ratio are the main parameters important for increasing the encapsulation efficiency of the nanoparticles, all five parameters included were part of a significant interaction term, as indicated to some extent in previous studies [17]. The explanations for the individual effects might be that the increased PLGA concentration results in a further stabilization of the primary emulsion and limits the diffusion of siRNA through and out of the organic phase due to the increased viscosity of the organic phase (see [Supplementary material](#)) and that a higher inner water phase volume reduces the concentration gradient between the inner and the outer water phase.

With respect to the sonication time, the siRNA and the Ac-BSA content included in the FFD, these factors do not by themselves pose significant differences, but synergistic effects in combination with other factors are observed. BSA has previously been used as a

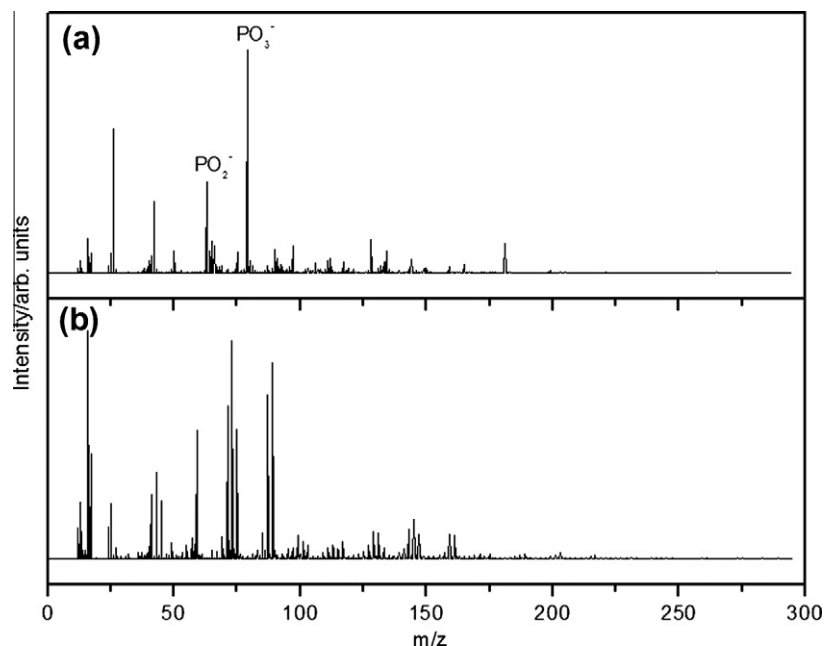


Fig. 4. Negative ToF-SIMS spectra acquired from (a) siRNA reference material and (b) placebo, non-loaded PLGA nanoparticles.

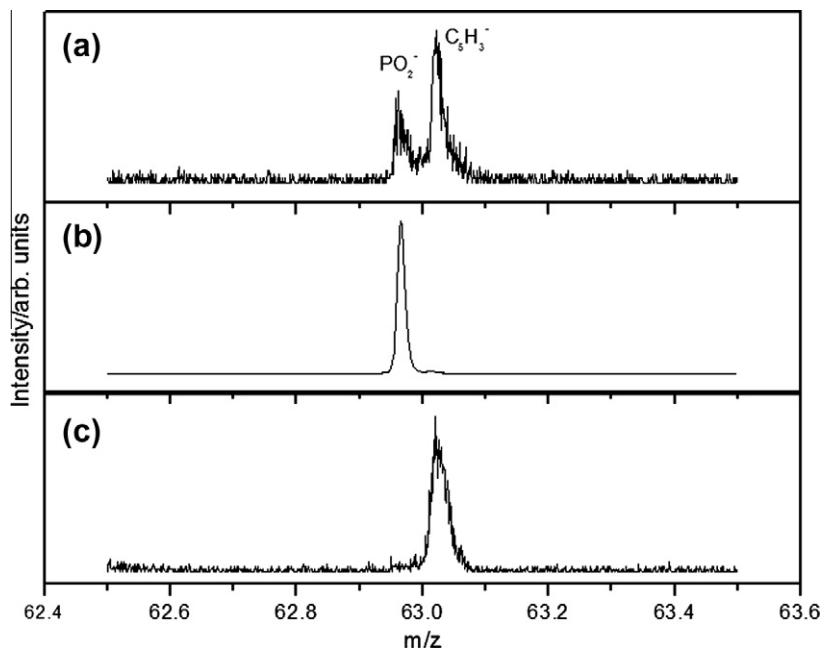


Fig. 5. Negative ToF-SIMS spectra at 63 m/z acquired from (a) siRNA-loaded PLGA nanoparticles, (b) siRNA reference material, and (c) placebo, non-loaded PLGA nanoparticles.

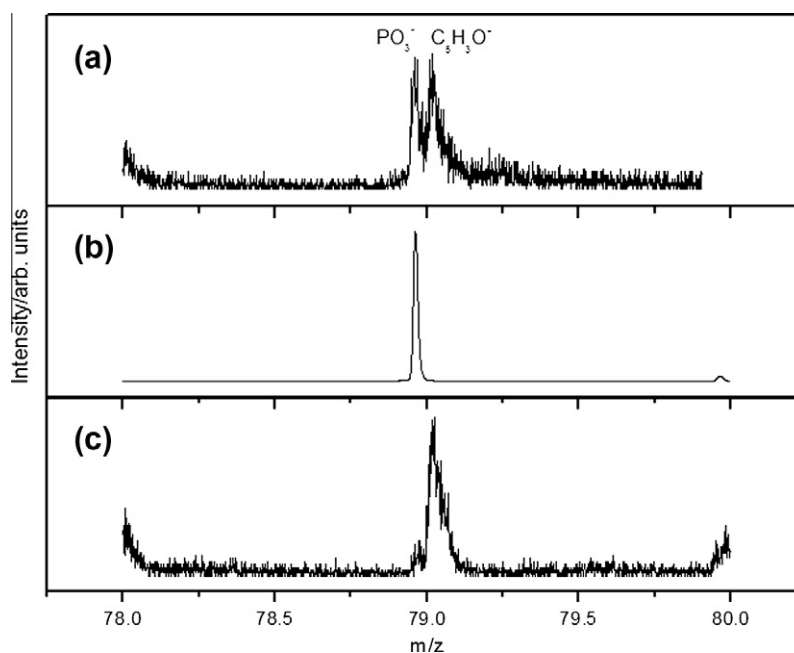


Fig. 6. Negative ToF-SIMS spectra at 79 m/z acquired from (a) siRNA-loaded PLGA nanoparticles, (b) siRNA reference material, and (c) placebo, PLGA nanoparticles.

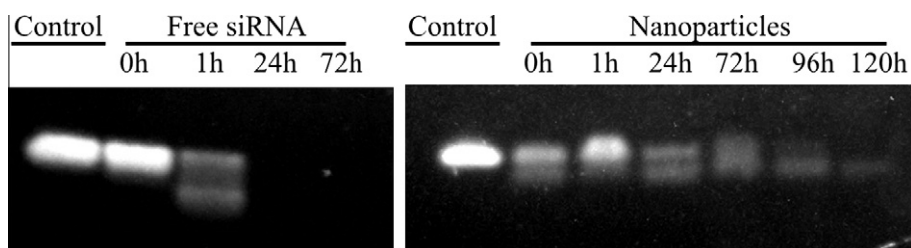


Fig. 7. Polyacrylamide gel electrophoresis of naked siRNA (left) and siRNA-loaded PLGA nanoparticles (right) incubated for different periods with Ribonuclease I “A” from bovine pancreas.

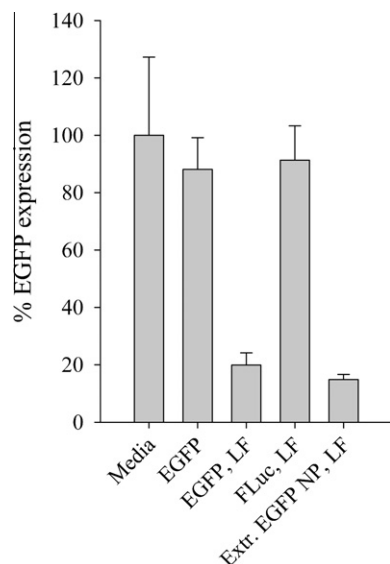


Fig. 8. Flow cytometry analysis of H1299 cells stably expressing EGFP after 48 h of incubation with siRNA extracted from PLGA nanoparticles (NP). siRNA co-administered with lipofectamine 2000 (LF) was used as the positive control, and siRNA targeting FLuc in the same concentrations as for the positive control administered together with lipofectamine 2000 was used as the negative control. The mean fluorescence intensity was normalized to the mean fluorescence intensity of medium-treated cells. Data represent mean \pm SD ($n = 3$).

co-excipient for encapsulation in PLGA particles due to its surfactant properties in order to stabilize the primary emulsion and reduce the risk of coalescence and thus the diffusion of siRNA into the outer water phase [20]. Therefore, the colloidal stabilization of the system is presumably of primary importance. The stabilizing effect of BSA is more prominent at low PLGA concentrations, whereas the effect is absent at high PLGA concentrations, indicating that the low concentration PLGA primary emulsions are less stable than the emulsions with high concentrations of PLGA. To increase the overall efficiency of siRNA and DNA nanoparticles, cationic complexing agents (such as PEI and poly-L-lysine) are often used successfully in the formulation process resulting in increased encapsulation efficiency as well as an increased surface charge. It is, however, evident that this affects the release profile [21,10]. Due to the potential toxicity induced by these cationic excipients [22], increasing encapsulation efficiency should be approached by other means, and the present studies consolidate that the encapsulation efficiency can be improved significantly to as much as 70% merely by process optimization.

The second validation parameter which is a very important physicochemical parameter for the efficacy of the drug delivery system *in vivo* is the particle size. The particle size is important for the *in vivo* distribution and cellular uptake, but can also affect the release profile of the drug from the particles, as smaller particles have a larger surface area. This might result in a high burst release of the drug and a shorter period of sustained release [23]. Generally, an overall increase in the mass of material used will increase the particle size [24], which is illustrated by the results that the concentration of PLGA is the primary variable responsible for the changes in particle size. However, it should be noted that in all batches prepared, the particle size ranged from 218 to 258 nm, which in all cases is considered suitable for cellular uptake.

Since the changing of the constituent in the w_2 phase could increase the particle size beyond the desired value [25–27], the concentration and amount of PVA introduced in the process was fixed to 2% (w/v) in the present study, as it has previously been shown sufficient, yet essential, in producing well-defined nanopar-

ticles [17]. It is possible that the alteration of the polymer concentration in the w_2 phase could increase the encapsulation efficiency without compromising the particle size [27].

A burst release is generally considered to result from the release of surface-associated siRNA. The presence of surface-associated siRNA was confirmed by ToF-SIMS analysis. ToF-SIMS is a highly surface sensitive, non-quantitative, spectroscopic technique, where only the first molecular monolayers of a sample are interrogated. The technique, which is performed under ultra-high vacuum conditions, has found use in a variety of biomedical applications, including biomaterials [28], identifying absorbed proteins [29] and DNA fragments [30], the detailed surface characterization of PLGA films [31] and PLGA microparticles [32]. ToF-SIMS analysis showed peaks assigned to the PO_2^- and PO_3^- ion fragments originating from surface-bound siRNA. The level of burst release in the present study was around 15%, which is lower than reported elsewhere [9,10], indicating that the major fraction of the siRNA is localized inside the nanoparticle matrix.

The observed change in release rate in the period after the burst release can be due to the distribution of siRNA inside the nanoparticle matrix or a change in matrix degradation rate [21] as a result of changed surface porosity and internal morphology, which have proven important parameters for the appearance of the release profile [25]. The siRNA release occurs over more than fifty days providing an attractive sustained release profile for this potent drug, where maintenance of a therapeutically relevant siRNA concentration for a prolonged time period is essential for many therapeutic regimes. Also, the overall release profile is not dependent on the level of siRNA loading.

From the RNase protection experiments, it is clear that the integrity of the siRNA is maintained for several days under enzymatically harsh conditions. Further, the functional activity of the siRNA seems to be preserved during the preparation of the nanoparticles by the gentle double emulsion solvent evaporation method, which is an additional indication that the optimal process parameters can be applied to prepare siRNA nanoparticles with remarkably high encapsulation efficiency, a size around 250 nm and a negative zeta potential.

We are currently investigating additional possibilities for improving the efficacy of the PLGA-based drug delivery system, with special focus on improving the cellular transfection efficiency.

5. Conclusion

This study demonstrates that it is possible to increase the encapsulation efficiency without the use of cationic co-excipients to more than 60–70% of biologically active siRNA by the choice of optimized formulation parameters without compromising the particle size and the negative particle zeta potential. By statistical design of experiments, the most important parameters were found to be the concentration of PLGA and the w_1/o phase ratio. In addition, the co-excipient Ac-BSA seems to have a positive effect on the level of encapsulation. The optimal formulation parameters were found to be a V_{w1}/V_o ratio of 0.4, a PLGA concentration of 60 mg/ml and an Ac-BSA concentration of 2 mg/ml for the loading of between 700 and 2200 ng siRNA/mg PLGA nanoparticle. siRNA was detectable on the surface of the nanoparticles and accounted for a burst release followed by a continuous triphasic release behavior of biologically active siRNA.

Acknowledgements

We are grateful to Maria Læssøe Pedersen and Stefania Baldursdottir for their excellent technical assistance. Brian Sproat is kindly acknowledged for the synthesis of the siRNA. We thank

the Alfred Benzon Foundation (D.C.), the Danish Research Council for Technology and Production Sciences Grant No. 26-02-0019 (D.M.K.J.), Drug Research Academy and the Danish Agency for Science, Technology and Innovation for financial support. In addition, this paper has been carried out with financial support from the Commission of the European Communities, Priority 3 “Nanotechnologies and Nanosciences, Knowledge Based Multi-functional Materials, New Production Processes and Devices” of the Sixth Framework Programme for Research and Technological Development (Targeted Delivery of Nanomedicine: NMP4-CT-2006-026668).

Appendix A. Supplementary material

Supplementary data associated with this article can be found, in the online version, at [doi:10.1016/j.ejpb.2010.11.008](https://doi.org/10.1016/j.ejpb.2010.11.008).

References

- [1] S.D. Putney, P.A. Burke, Improving protein therapeutics with sustained-release formulations, *Nat. Biotechnol.* 16 (1998) 153–157.
- [2] R.C. Mundargi, V.R. Babu, V. Rangaswamy, P. Patel, T.M. Aminabhavi, Nano/micro technologies for delivering macromolecular therapeutics using poly(D,L-lactide-co-glycolide) and its derivatives, *J. Controlled Release* 125 (2008) 193–209.
- [3] Y. Ogawa, H. Okada, T. Heya, T. Shimamoto, Controlled release of LHRH agonist, leuprolide acetate, from microcapsules – serum drug level profiles and pharmacological effects in animals, *J. Pharm. Pharmacol.* 41 (1989) 439–444.
- [4] H. Okada, One- and three-month release injectable microspheres of the LH-RH superagonist leuporelin acetate, *Adv. Drug Deliv. Rev.* 28 (1997) 43–70.
- [5] D. Cun, L.B. Jensen, H.M. Nielsen, M. Moghimi, C. Foged, Polymeric nanocarriers for siRNA delivery: challenges and future prospects, *J. Biomed. Nanotechnol.* 4 (2008) 258–275.
- [6] M.J. Campolongo, D. Luo, Old polymer learns new tracts, *Nat. Mater.* 8 (2009) 447–448.
- [7] H. Cohen, R.J. Levy, J. Gao, I. Fishbein, V. Kousaev, S. Sosnowski, S. Slomkowski, G. Golomb, Sustained delivery and expression of DNA encapsulated in polymeric nanoparticles, *Gene Ther.* 7 (2000) 1896–1905.
- [8] J. Lutten, C.F. van Nostruijn, S.C. De Smedt, W.E. Hennink, Biodegradable polymers as non-viral carriers for plasmid DNA delivery, *J. Controlled Release* 126 (2008) 97–110.
- [9] K. Tahara, T. Sakai, H. Yamamoto, H. Takeuchi, Y. Kawashima, Establishing chitosan coated PLGA nanosphere platform loaded with wide variety of nucleic acid by complexation with cationic compound for gene delivery, *Int. J. Pharm.* 354 (2008) 210–216.
- [10] Y. Patil, J. Panyam, Polymeric nanoparticles for siRNA delivery and gene silencing, *Int. J. Pharm.* 367 (2009) 195–203.
- [11] K.A. Woodrow, Y. Cu, C.J. Booth, J.K. Saucier-Sawyer, M.J. Wood, W. Mark Saltzman, Intravaginal gene silencing using biodegradable polymer nanoparticles densely loaded with small interfering RNA, *Nat. Mater.* 8 (2009) 526–533.
- [12] U. Bilati, E. Allemann, E. Doelker, Poly(D,L-lactide-co-glycolide) protein-loaded nanoparticles prepared by the double emulsion method – processing and formulation issues for enhanced entrapment efficiency, *J. Microencapsul.* 22 (2005) 205–214.
- [13] C. Yan, J.H. Resau, J. Hewetson, M. West, W.L. Rill, M. Kende, Characterization and morphological analysis of protein-loaded poly(lactide-co-glycolide) microparticles prepared by water-in-oil-in-water emulsion technique, *J. Controlled Release* 32 (1994) 231–241.
- [14] H.K. Sah, R. Toddywala, Y.W. Chien, Biodegradable microcapsules prepared by a w/o/w technique – effects of shear force to make a primary w/o emulsion on their morphology and protein release, *J. Microencapsul.* 12 (1995) 59–69.
- [15] B. Singh, R. Kumar, N. Ahuja, Optimizing drug delivery systems using systematic “Design of experiments.” Part I: Fundamental aspects, *Crit. Rev. Ther. Drug Carrier Syst.* 22 (2005) 27–105.
- [16] B. Singh, M. Dahiya, P. Saharan, N. Ahuja, Optimizing drug delivery systems using systematic “Design of experiments.” Part II: Retrospect and prospects, *Crit. Rev. Ther. Drug Carrier Syst.* 22 (2005) 215–293.
- [17] D. Cun, C. Foged, M. Yang, S. Frokjaer, H.M. Nielsen, Preparation and characterization of poly(D,L-lactide-co-glycolide) nanoparticles for siRNA delivery, *Int. J. Pharm.* 390 (2010) 70–75.
- [18] D.M. Jensen, D. Cun, M.J. Maltesen, S. Frokjaer, H.M. Nielsen, C. Foged, Spray drying of siRNA-containing PLGA nanoparticles intended for inhalation, *J. Controlled Release* 142 (2010) 138–145.
- [19] C.J. May, H.E. Canavan, D.G. Castner, Quantitative X-ray photoelectron spectroscopy and time-of-flight secondary ion mass spectrometry characterization of the components in DNA, *Anal. Chem.* 76 (2004) 1114–1122.
- [20] D. Blanco, M.J. Alonso, Protein encapsulation and release from poly(lactide-co-glycolide) microspheres: effect of the protein and polymer properties and of the co-encapsulation of surfactants, *Eur. J. Pharm. Biopharm.* 45 (1998) 285–294.
- [21] J.S. Blum, W.M. Saltzman, High loading efficiency and tunable release of plasmid DNA encapsulated in submicron particles fabricated from PLGA conjugated with poly-L-lysine, *J. Controlled Release* 129 (2008) 66–72.
- [22] H. Lv, S. Zhang, B. Wang, S. Cui, J. Yan, Toxicity of cationic lipids and cationic polymers in gene delivery, *J. Controlled Release* 114 (2006) 100–109.
- [23] R. Singh, J. Lillard, Nanoparticle-based targeted drug delivery, *Exp. Mol. Pathol.* 86 (2009) 215–223.
- [24] M.N.V.R. Kumar, U. Bakowsky, C.M. Lehr, Preparation and characterization of cationic PLGA nanospheres as DNA carriers, *Biomaterials* 25 (2004) 1771–1777.
- [25] S.R. Mao, J. Xu, C.F. Cai, O. Germershaus, A. Schaper, T. Kissel, Effect of WOW process parameters on morphology and burst release of FITC-dextran loaded PLGA microspheres, *Int. J. Pharm.* 334 (2007) 137–148.
- [26] M.L. Zweers, D.W. Grijpma, G.H. Engbers, J. Feijen, The preparation of monodisperse biodegradable polyester nanoparticles with a controlled size, *J. Biomed. Mater. Res. B Appl. Biomater.* 66 (2003) 559–566.
- [27] J. Vandervoort, A. Ludwig, Biocompatible stabilizers in the preparation of PLGA nanoparticles: a factorial design study, *Int. J. Pharm.* 238 (2002) 77–92.
- [28] A.M. Belu, D.J. Graham, D.G. Castner, Time-of-flight secondary ion mass spectrometry: techniques and applications for the characterization of biomaterial surfaces, *Biomaterials* 24 (2003) 3635–3653.
- [29] J.B. Lhoest, M.S. Wagner, C.D. Tidwell, D.G. Castner, Characterization of adsorbed protein films by time of flight secondary ion mass spectrometry, *J. Biomed. Mater. Res. Part A* 57 (2001) 432–440.
- [30] H.F. Arlinghaus, M. Ostrop, O. Friedrichs, J. Feldner, U. Gunst, D. Lipinsky, DNA sequencing with ToF-SIMS, *Surf. Interface Anal.* 34 (2002) 35–39.
- [31] R. Ogaki, A.G. Shard, S.M. Li, M. Vert, S. Luk, M.R. Alexander, I.S. Gilmore, M.C. Davies, Extracting information on the surface monomer unit distribution of PLGA by ToF-SIMS, *Surf. Interface Anal.* 40 (2008) 1168–1175.
- [32] J. Chesko, J. Kazzaz, M. Ugozzoli, M. Singh, D.T. O’Hagan, C. Madden, M. Perkins, N. Patel, Characterization of antigens adsorbed to anionic PLG microparticles by XPS and TOF-SIMS, *J. Pharm. Sci.* 97 (2008) 1443–1453.